construction materials

MDPI

Article

Stress–Strain State and Strength of Fiber-Reinforced Concrete Beams with Basalt, Steel, and Polypropylene Fibers

Abdurasul Martazaev * and Sobirjon Razzakov

Department of Construction of Buildings and Structures, Faculty of Construction, Namangan State Technical University, Namangan 160103, Uzbekistan; sobirjonrsj@gmail.com
* Correspondence: abdurasul.mas@gmail.com

Abstract

Fiber-reinforced concrete has proved to be viable in improving the mechanical characteristics of structural elements to the flexural and shear stresses. The concrete cubes, prisms, and cylinders were standardized, cast and cured after 28 days to assess the baseline mechanical characteristics. Beam specimens were made of different types of fibers, lengths, and different volumetric contents and then subjected to controlled shear tests in which the crack initiation, propagation, and deformation were accurately measured. The experimental data proved that the addition of fibers was highly beneficial in terms of the mechanical performance of concrete. Basalt fibers enhanced compressive strength by up to 20.8 percent and tensile strength by 30.8 percent, whereas steel fibers had the best flexural strength with a maximum compressive and bending strength of 47.2 MPa and 6.56 MPa, respectively, at optimum dosage. Polypropylene fibers also improved performance, but in a lesser manner. The fiber addition served well to reduce the width of cracks and retard crack propagation, thus enhancing load-bearing capacity. These results show that dispersed fiber reinforcement that uses steel and basalt fibers is a practical solution to improving the dispersion of concrete in terms of durability and load-bearing capacity. The research will help guide the selection of fiber and the content in the reinforced concrete work to offer more robust and sustainable solutions to building.

Keywords: fiber-reinforced concrete; basalt fibers; steel fibers; polypropylene fibers; shear strength

1. Introduction

Concrete are one of the most popular structural materials of the present civil engineering practice because of the favorable combination of mechanical characteristics, durability, and cost-effectiveness [1]. They are widely used in buildings, bridges, industrial structures and transport structures where they mostly experience flexural loading. Although they are widely used, conventional reinforced concrete beams have a number of shortcomings inherent to them at the time when they are under bending moments [2]. These shortcomings consist of premature tensile cracking, high rate of crack growth, low post tensile cracking hardness and comparatively brittle failure behavior after tensile reinforcement yields. The implications of such limitations have negative impacts on the end load-bearing capacity in addition to serviceability performance, durability, and reliability of reinforced concrete structures [3]. The tensile strength of concrete is very low and therefore the tensile zone of a reinforced concrete beam is especially susceptible to flexural loading [4]. After the tensile stress reaches the cracking threshold, discrete cracks develop and propagate very

Check for updates

Received: 27 December 2025
Revised: 3 March 2026
Accepted: 20 March 2026
Published: 25 March 2026

Copyright: © 2026 by the authors. Licensee MDPI, Basel, Switzerland. This article is an open access article distributed under the terms and conditions of the Creative Commons Attribution (CC BY) license.

fast, resulting in stress concentration and loss in stiffness [5]. Despite the traditional steel reinforcement with tensile forces being efficiently expressed after cracking, the concrete between cracks loses much of its tension strength, leaving large apertures on the cracks and lowering the stability of the structure [6]. In addition, its stress–strain behavior of the traditional RC beams is that the transition between elastic and cracked phases is sharp and the beam has limited energy dissipation capacity and collapses abruptly in some situations [7]. These problems are acute in the case of high loads of services, dynamic or cyclic loading, and in harsh environmental conditions [8].

The author has introduced the methods of strengthening and improving its characteristics to eliminate these shortcomings, however in particular, dispersion in fiber reinforcement has been of interest over the past decades [9]. Improvement of the material behavior involves the use of the short, discrete fibers into the concrete matrix to provide an added crack-bridging mechanism [10]. In contrast to the traditional reinforcement bars that work at the macro-scale only, the dispersed fibers are in place at random all through the concrete volume and the interaction with micro- and macro-cracks at various loading stages takes place [11]. This multiscale reinforcement mechanism allows better crack management, better redistribution of stress and delayed crack coalescence, and thus has a significant impact on the stress–strain curve and failure behavior of reinforced concrete members. The principle of dispersed reinforcement is anchored on the fact that fibers can transmit tensile forces across cracks using interfacial bonding, friction and mechanical anchorage [12]. As the microcracks commence in the concrete matrix, the fibers which cross the microcracks inhibit their cracking and retard the speed at which they widen. As the loading is increased and the cracks evolve into macro-cracks, the fibers will continue to bridge the surfaces of the cracks to give the remaining tensile capacity and increase the post-cracking stiffness. This is a mechanism that causes a slower process of stiffness degradation, greater deformation capacity and enhanced energy absorption [13]. The FRC beam is therefore more ductile, toughened and damage-tolerant than the traditional RC beam.

Out of all the different types of fibers used in dispersed reinforcement, steel, polypropylene and basalt fibers have become the most frequently used fibers because of their availability, cost-effectiveness and mechanical properties specific to them [14]. The tensile strength, elastic modulus, geometry, and surface properties as well as interaction with the cementitious matrix of each type of fiber play different roles in the stress–strain behavior and structural performance of reinforced concrete beam. Steel fibers are commonly described in terms of high tensile strength and great elastic modulus that makes them effective especially in flexural strength as well as load bearing [15,16]. They offer good crack-bridging behavior, and consequently, increase in stiffness during the post-cracking stage and have a great increase in residual strength [17]. Many experiments have shown that metal-reinforced concrete beams using the steel fibers show less spacing between cracks, small crack widths, and the ability to dissipate a lot of energy. But steel fibers can be easily corroded in harsh conditions and as such, long life durability can be affected unless proper protection is provided [18].

Polypropylene fibers on the other hand have relatively low tensile strength and elastic modulus in comparison to steel fibers [19]. In spite of this, PP fibers are important in managing cracking of plastic shrinkage and formation of microcracks at an early age. Their deformation capacity and their low density are some factors that make concrete elements to have better ductile and strain capacity [20]. The benefit of PP fibers is that in flexural members, the deformation capacity and post-cracking performance are improved, although their ultimate strength is usually small [21]. The polypropylene fibers are especially appealing to use where durability and long-term performance become a major concern owing to their chemical inertness and resistance to corrosion [22]. Recently, basalt fibers,

which are made of natural basalt rock, are facing a lot of attention as an alternative material that can replace the traditional fibers as sustainable and high-performance. Basalt fibers have great tensile strength, comparatively high elastic modulus, high thermal stability, and high resistance to chemical attack and corrosion [23]. In addition, they have less environmental effects in their production as opposed to synthetic fibers and are therefore environmentally friendly [24]. Basalt fiber has shown potential in reinforced concrete beams as a promising tool for better control of cracks, better flexural behaviors and post-cracking behaviors [25]. But their performance is highly bound on the length of fibers, volume fraction and the bonding with cementitious matrix [26].

Although there has been an extensive amount of literature on fiber-reinforced concrete, the majority of current studies are either on a single type of fiber or examine fibers under different environmental conditions, including the different concrete compositions, reinforcement configurations, or loading configurations [27]. Therefore, direct comparisons of the various types of fibers tend to be inconclusive [28]. Specifically, the overall assessment of the stress–strain state of reinforced concrete beams reinforced with dispersedly reinforced steel, polypropylene, and basalt fibers under the same experimental conditions is under-researched [29,30]. Numerous investigations focus on ultimate load capacity or cracking patterns, and there is a relative paucity of studies that analyze the distribution of strains, degradation of stiffness, post-yield behavior, and mechanisms of failure [31,32].

Moreover, the interactions between the traditional reinforcement bars and dispersed fibers are complicated, thus affecting the general structural reaction greatly. The fibers change the tensile characteristics of concrete, crack spacing, and width, as well as influence the stress transfer process between concrete and steel reinforcement [33]. The effect differs according to the type of fiber and its mechanical properties. Thus, a single experimental design that would offer comparative analysis of the various types of fibers is needed to provide credible design guidelines and to improve the feasibility of using fiber-reinforced concrete in structural engineering.

It is against this backdrop that the current research paper aims to fill the research gap by undertaking comparative experimental research on the stress–strain behavior and strength of reinforced concrete beams incorporating basalt, steel, and polypropylene fibers [34]. The beam specimens have the same geometry and reinforcement layout, concrete mixture, and curing condition so as to provide a fair comparison. The main research hypotheses are that the incorporation of dispersed basalt, steel, and polypropylene fibers will increase the flexural and shear performance of reinforced concrete beams over plain reinforced concrete beams, that different fiber types, lengths, and volume fractions have different effects on crack initiation, propagation, and post crack ductility, and that the use of traditional reinforcement bars and dispersed fibers on the beams will have an interaction effect on the stress–strain response of the beams, crack spacing, and stress transfer. According to these hypotheses, the experimental program is used to measure the load-deflection behavior, the strain distribution of concrete as well as the reinforcement, the crack initiation and propagation, flexural strength, and failure mechanisms. The originality of this study is found in the structural comparison of three fundamentally varying types of fibers under unified experimental conditions, which provide good information on how the best type of fiber can be selected based on a certain performance requirement, durability factor and even sustainability goal.

2. Materials and Methods

2.1. Construction of the Testing Samples

For the experimental investigation, beam specimens were prepared in four series. The first series comprised control specimens comprising traditional concrete that was not

fiber-reinforced. The beams were made by the use of Portland cement, fine and coarse aggregates and water without using fibers. The specimens that were used as the control were the reference samples that were used in the comparison with the fiber reinforced concrete beams. The distribution of sample beams by fiber type, quantity, and length is presented in Table 1.

Table 1. Experimental program and details of fiber-reinforced concrete specimens.

No.	Series	Designation	Fiber Type	Fiber Length (mm)	Fiber Content (%)	Number of Specimens
1	S1 (Control)	BO	(Plain concrete)	-	-	3
2	S2	BB10-0.1	Basalt	10	0.1	3
3		BB10-0.2	Basalt	10	0.2	3
4		BB10-0.3	Basalt	10	0.3	3
5		BB30-0.1	Basalt	30	0.1	3
6		BB30-0.2	Basalt	30	0.2	3
7		BB30-0.3	Basalt	30	0.3	3
8	S3	BP10-0.1	Polypropylene	10	0.1	3
9		BP10-0.2	Polypropylene	10	0.2	3
10		BP10-0.3	Polypropylene	10	0.3	3
11		BP30-0.1	Polypropylene	30	0.1	3
12		BP30-0.2	Polypropylene	30	0.2	3
13		BP30-0.3	Polypropylene	30	0.3	3
14	S4	BS30-1.0	Steel	30	1.0	3
15		BS30-2.0	Steel	30	2.0	3
16		BS30-3.0	Steel	30	3.0	3

In the second series, basalt fiber-reinforced concrete beam specimens were prepared. Basalt fibers with two different lengths (10 mm and 30 mm) were incorporated into the concrete mixture at volumetric contents of 0.1%, 0.2%, and 0.3%. For each fiber length and dosage, three beam specimens were cast, resulting in a total of 18 basalt fiber-reinforced concrete beams. The third series included polypropylene fiber-reinforced concrete beams. Polypropylene fibers with lengths of 10 mm and 30 mm were added to the concrete at the same volumetric contents of 0.1%, 0.2%, and 0.3%. Similarly, three beam specimens were prepared for each combination, yielding a total of 18 polypropylene fiber-reinforced concrete beams. In the fourth series, steel fiber-reinforced concrete beams were produced. Steel fibers with a length of 30 mm were added to the concrete mixture at volume fractions of 1%, 2%, and 3%. For each fiber content, three beam specimens were prepared, resulting in a total of 9 steel fiber-reinforced concrete beams.

Specimens of reinforced concrete beams were made of steel, basalt, and polypropylene fiber-reinforced concrete, having dimensions 100 × 200 × 1200 mm.

Longitudinal reinforcement was made up of two deformed reinforcing bars having a diameter of 12 mm, and they were A-III grade steel. The longitudinal reinforcement ratio of the beams was 1.33 percent.

The transverse reinforcement was done with the stirrups that were made of B-I grade steel wire, 5 mm in diameter. The spacing between the stirrups was 60 mm where the beam was supported and 90 mm at the midspan as indicated in Figure 1.

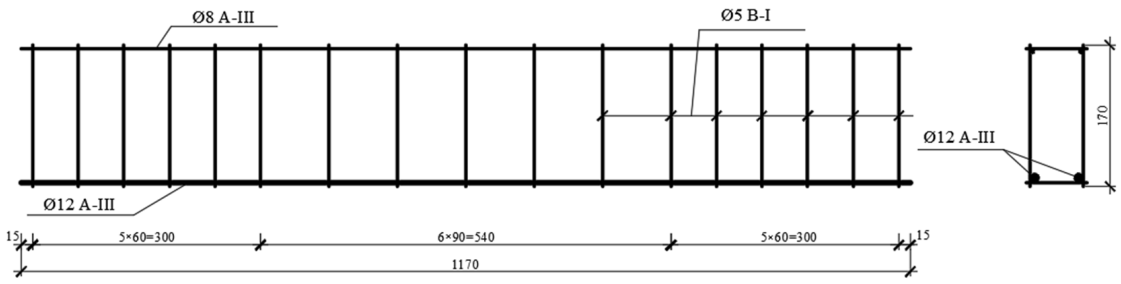


Figure 1. Beam reinforcement scheme.

2.2. Materials

Cement is another major component of concrete and has a direct impact on the mechanical performance of concrete. The cement Portland PS400D20 (Namangan sement LTD, Chust, Uzbekistan) of the plant called Namangansement was used in this study. The true density of the cement was 3.1 g/cm^3, the bulk density was 1.3 g/cm^3, the standard consistency was 26 percent, the fineness residue was 8.2 percent and the specific surface area was between 3000 and 3500 cm^2/g. The flexural strength and compressive strength (28 days) of the cement was 43.0 MPa and 7.1 MPa respectively.

The fine aggregate was natural sand which was obtained in Namangan region, Toraqorgon district and quarry at Namangan. The density of the sand was 2670 kg/m^3, the size of the particles was 0–5 mm, and the moisture content was 3.1%. The coarse aggregate was crushed granite, with a density of 2665 kg/m^3 and a range of particle size (5–20 mm).

To reinforce the concrete, it was dispersed with steel fibers with a length of 30 mm and a diameter of 0.3 mm. The density of the steel fibers was 7850 kg/m^3, tensile strength of 1100 MPa, and the elastic modulus of 200 GPa. Moreover, basalt fibers produced by the Basalt Uzbekistan Joint Venture were also used which is situated in the Jizzakh region of Uzbekistan. Basalt fibers were 2650 kg/m^3 in density, 3500 MPa in tensile strength, 110 GPa in elastic modulus, 17 μm in fiber diameter, and 30 mm in length.

They were also made in polypropylene with a density of 910 kg/m^3, tensile strength of 500 MPa, elastic modulus of 35 GPa, fiber diameter of 18 μm and fiber length 10 mm and 30 mm. Table 2 shows the physical properties of fibers used in this study.

Table 2. Physical and mechanical properties of fibers.

Fiber Type	Density (kg/m^3)	Tensile Strength (MPa)	Elastic Modulus (GPa)	Fiber Length (mm)	Fiber Diameter (mm)
Basalt	2650	3500	110	10, 30	0.017
Polypropylene	910	500	35	10, 30	0.018
Steel	7850	1100	200	30	0.3

The concrete mix used for the preparation of all beam specimens consisted of 440 kg of cement, 1025 kg of fine aggregate, 815 kg of coarse aggregate, and 180 L of water, resulting in a water-to-cement ratio of 0.41. All fibers were added according to the type, volume fraction, and length specified for each series.

According to the demands of [35], physical and mechanical properties of the concrete were carried out based on standard cube, prism and cylinder specimens casted with the same batch of concrete used on the experimental beams. The tests to be measured on the concrete specimens were performed at the age of 28 days—both prior to testing of the experimental beams and by the time of all beam tests being completed. All tests were performed in a hydraulic press SYE-2000 (IN-TEST, China). The residual tensile strength values reported in Table 3 were obtained according to the standard procedure described in

"Fiber reinforced concrete structures and precast products with non-steel fibers," Design rules DR297.1325800.2017 [36]. Table 3 shows the experimentally obtained physical and mechanical properties of concrete based on the cube, prism and cylinder tests. These findings will serve as a benchmark in the assessment of the behavior of the fiber-reinforced concrete beams.

Table 3. Mechanical properties of samples dispersed reinforced with fibers.

Designation	Compressive Strength (MPa)	Tensile Strength (MPa)	Residual Tensile Strength (MPa)	Flexural Strength (MPa)	Elastic Modulus (GPa)
BO	34.6	2.21	–	4.41	30.91
BB10-0.1	40.7	2.81	1.16	5.52	34.9
BB10-0.2	41.8	2.89	1.29	5.81	35.4
BB10-0.3	39.9	2.68	1.19	5.49	34.2
BB30-0.1	39.8	2.66	1.21	5.61	33.7
BB30-0.2	41.1	2.87	1.32	5.76	35.0
BB30-0.3	40.2	2.74	1.26	5.68	34.1
BP10-0.1	38.6	2.71	1.25	5.54	34.6
BP10-0.2	39.9	2.76	1.20	5.73	34.8
BP10-0.3	38.2	2.69	1.12	5.30	33.4
BP30-0.1	39.7	2.78	1.23	5.62	35.1
BP30-0.2	38.9	2.72	1.18	5.42	34.6
BS30-0.3	38.1	2.65	1.10	5.31	34.1
BS30-1.0	45.1	3.48	1.62	6.42	35.6
BS30-2.0	47.2	3.54	1.75	6.56	36.8
BS30-3.0	44.3	3.10	1.53	6.33	34.8

Dispersed fiber reinforcement greatly enhanced the mechanical properties of fiber-reinforced concrete specimens. In compressive strength, control specimen (BO) had a compressive strength of 34.6 MPa with the basalt fiber-reinforced specifications of 39.8–41.8 MPa with the greatest strength of 41.8 MPa which is a 20.8 percentage improvement. The tensile strength had risen to 2.66–2.89 MPa in basalt fiber specimens as compared to 2.21 MPa in plain concrete and the improvement in BB10-0.2 was 30.8%. Remaining tensile strength of 10 mm specimens with basalt fibers (basalt fibers) was between 1.16 and 1.29 MPa and 1.19 and 1.32 MPa in 30 mm fiber specimens. It also enhanced flexural strength, which was 4.41 MPa in the control and 5.49–5.81 MPa in the basalt fiber specimen, which is an increment of 25 to 32 percent.

Fiber-reinforced polypropylene was also used to improve concrete performance. Compressive, tensile, and flexural strengths of BP10-0.1 and BP10-0.2 were 38.6 and 39.9 MPa, 2.71 and 2.76 MPa and 1.12–1.25 times greater than plain concrete respectively. Similar improvements were demonstrated by BP30 series. Mechanical performance was best exhibited by steel fiber-reinforced beam. Compressive strengths of 1, 2 and 3 percent steel fiber beam were 45.1, 47.2 and 44.3 MPa respectively and tensile strengths rose to 3.48–3.54 MPa. Flexural strengths were at 6.33–6.56 MPa and the increase in elastic modulus was as 30.91 GPa to 35.6–36.8 GPa. All in all, the highest results of compressive, tensile, and flexural performances were found among steel fiber-reinforced specimens, then basalt fiber and polypropylene fiber specimens.

2.3. Testing Methodology

In the tests, the loads were uniform and applied symmetrically to all the beams. The supports were used with 75 mm distance between the beam ends and the loads were applied 262 mm between the supports and the distance between the points was 526 mm. Precise testing was done before by measuring the geometric dimensions of each beam. The

lateral sides of the beams were painted white to make it easy to observe the cracks and a position of the cage of reinforcements was marked. The dial gauges and deflectometer were used to measure the relative deformations in the concrete and reinforcement with a tolerance of 0.001 mm. The loading diagram of the sample beams is shown in Figure 2.

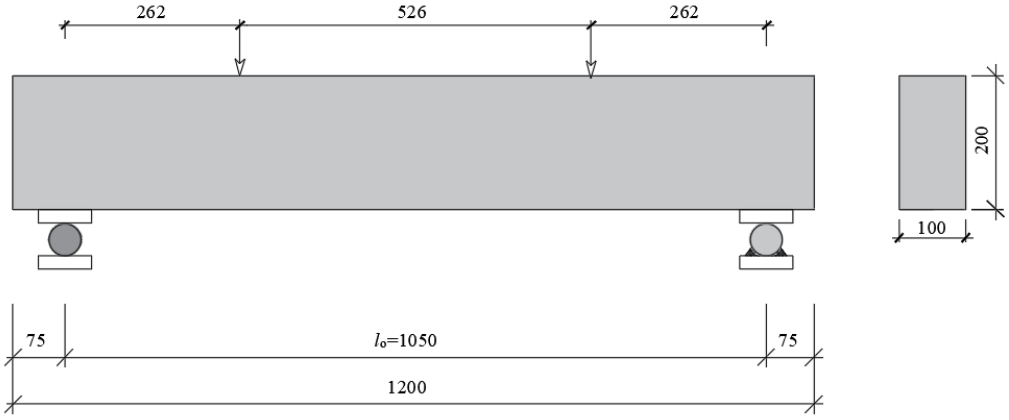


Figure 2. Sample beam loading scheme.

The load was put on in stages. First, the load that was not more than 5 percent of the ultimate load that was computed was placed before the development of the cracks. Three more steps added the load in steps no longer than 10 percent of the final load, whereby the crack propagation and beginning could be closely observed. All the cracks were numbered, and their length, orientation, and location with regard to the reinforcement were taken. Once the applied load was about 85–90 percent of the final load, measurement equipment was removed carefully so as not to cause any damage. The loading process was carried on till the beam failed completely and the process of failure was observed visually. The process of testing the strength of reinforced concrete beams in a shear section is shown in Figure 3.

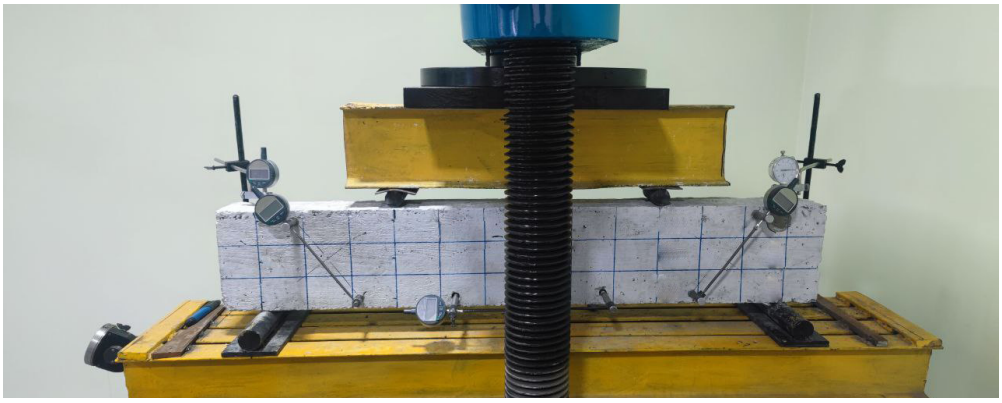


Figure 3. The process of testing the strength of reinforced concrete beams in shear sections.

The test results were very informative on the initiation and development of the crack, ultimate bending moment, failure load and deflection properties. With the help of these observations, a quantitative evaluation of the performance of the beams reinforced with various types and quantities of fibers was possible, which gave information on the performance of the beams in terms of the ability to control cracks, flexural strength, and the effectiveness of the whole structure.

3. Results

3.1. Formation and Development of Cracks in the Shear Section of Fiber-Reinforced Concrete Beams

Shear observation of reinforced concrete beam showed that fiber-reinforced and non-fiber-reinforced specimens had distinct differences in the shear behavior during the failure process. The shear section failed in all the beams that were tested. The diagonal cracks that formed in the control reinforced concrete beam with no fibers were mainly formed in the areas surrounding the supports and extended at a forty-five-degree angle. At the point of the maximum load, these beams collapsed abruptly in a brittle fashion, which meant that they had very little post-cracking strength.

On the contrary, beams that had basalt, polypropylene and steel fiber reinforcement had a very different cracking behavior. The inclusion of fibers was key in limiting the crack initiation and propagation by limiting the widening of cracks, decreasing the separation between the cracks and slowing down the general failure. This made fiber-reinforced beams retain some amount of load-bearing capacity despite development of diagonal cracks. Figures 4–7 shows the observed pattern of cracking and mode of failure of the beams.

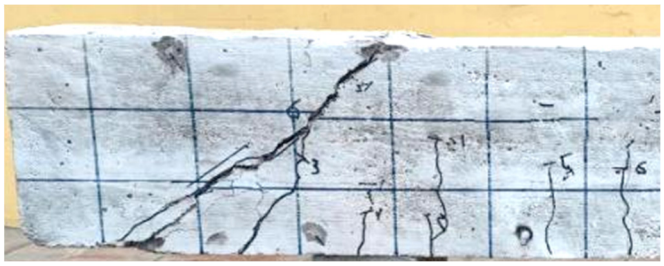


Figure 4. Formation of shear cracks in samples from the S1 series.



Figure 5. Formation of shear cracks in samples from the S2 series.



Figure 6. Formation of shear cracks in samples from the S3 series.

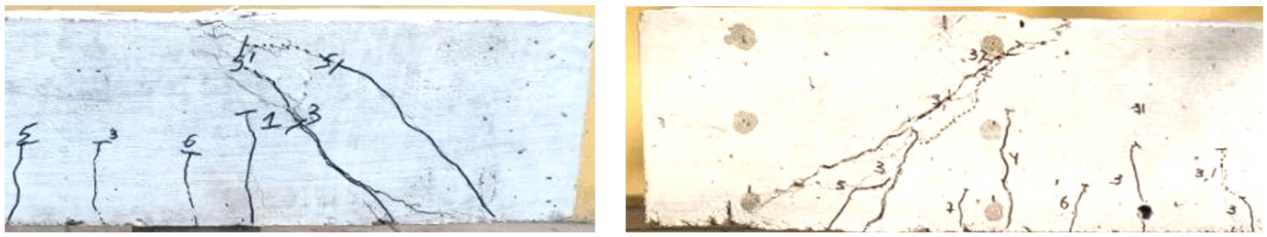


Figure 7. Formation of shear cracks in samples from the S4 series.

The results obtained allowed assessing the effect of fiber type, dosage, and length on the formation and growth of normal cracks and inclined cracks in reinforced concrete beams under shear dominated loading. Table 4 summarizes the moments due to normal cracking (M_{crc}) and the shear forces due to the generation of the first inclined crack (Q_{crc}) and the width of the crack at 50 of the ultimate load.

Table 4. Moments causing normal and oblique cracks in sample beams.

Series	ID	M_{crc}, (kN·m)	Q_{crc}, (kN)	Crack Width at 50% Q_{max}, (mm)
S1 (Control)	BO	2.69	32.23	0.37
S2	BB10-0.1	4.37	41.97	0.21
	BB10-0.2	4.46	42.12	0.19
	BB10-0.3	4.02	39.06	0.22
	BB30-0.1	4.09	38.92	0.20
	BB30-0.2	4.25	40.69	0.18
	BB30-0.3	3.90	39.87	0.25
S3	BP10-0.1	3.80	38.05	0.21
	BP10-0.2	3.99	41.14	0.24
	BP10-0.3	3.92	38.28	0.26
	BP30-0.1	4.01	40.49	0.20
	BP30-0.2	3.87	39.10	0.25
	BS30-0.3	3.81	38.56	0.20
S4	BS30-1.0	4.60	52.59	0.15
	BS30-2.0	5.00	54.42	0.10
	BS30-3.0	4.71	48.62	0.12

Generally, all fiber-reinforced specimens showed a delayed crack initiation and better crack management than those of the control beam (BO). The series were taken into account in the case of polypropylene fiber-reinforced beams BP10 and BP30, which are the fiber lengths of 10 mm and 30 mm, respectively. There was a steady increment of normal cracking moment and oblique cracking shear force in the BP10 series compared to controls beam. Table 4 showed that M_{crc} and Q_{crc} of BP10 were greater than Assays of BO, which proves that polypropylene fibers also help in postponing flexural crack initiation, as well as the formation of diagonal cracks.

The strongest enhancement in the BP10 category was seen in BP10-0.2 which means a moderate amount of fiber dose offers a better crack-bridging mechanism than either less or more of a dosage. This is due to improved dispersion of the fibers and less likelihood of localization that enhances the redistribution of stress across the microcracks before a dominant inclined crack is formed. The graphs of forces and moments causing cracks in the beams are shown in Figure 8.

On the same note, the BP30 series (30 mm fibers) had higher resistance to crack than the control specimen. M_{crc} and Q_{crc} increase was typically similar to that of the BP10 series but the variations between the 10 mm and 30 mm polypropylene fibers were not as intense as those found in the case of steel fiber reinforcement. The findings indicate that polypropylene fibers are primarily involved in the control of early cracks and serviceability performance, and not the maximum shear resistance, which is expected given their low elastic modulus. Moreover, the crack width at half of Q_{max} was also significantly lower in brittle polypropylene fiber beam relative to BO, which signified a better post-cracking performance and more capacity to bridge the cracks in tilted crack section.

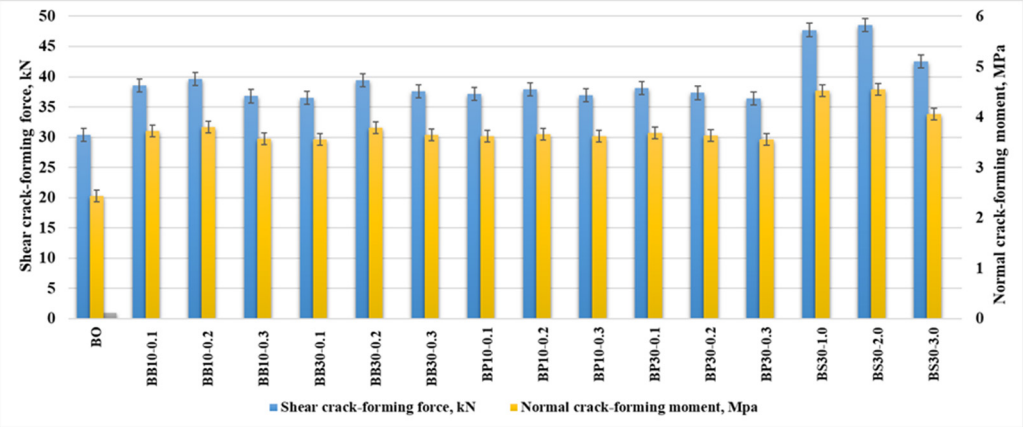


Figure 8. Graph of forces and moments that cause shear cracks in beams.

It was found that steel fiber-reinforced beams (BS30 series) had the most significant growth in crack resistance compared to all other types of fiber tested. All dosage levels (1 to 3 percent) of steel fiber in the beam showed significant increase in both M_{crc} and Q_{crc} compared to the control beam. The highest performance was recorded in the case of 2% steel fiber volume fraction (BS30-2.0) in which the highest cracking moment and the maximum shear force that the first inclined crack corresponds to are recorded (Table 4). The action reinforces the better contribution of steel fibers to the effect of shear transfer of the fibers, such as bridging the diagonal cracks, the increased interlock between the aggregates, and the strengthening of the dowel effect of longitudinal reinforcement. The width of opening of shear cracks in the sample beams is presented in Figures 9–12.

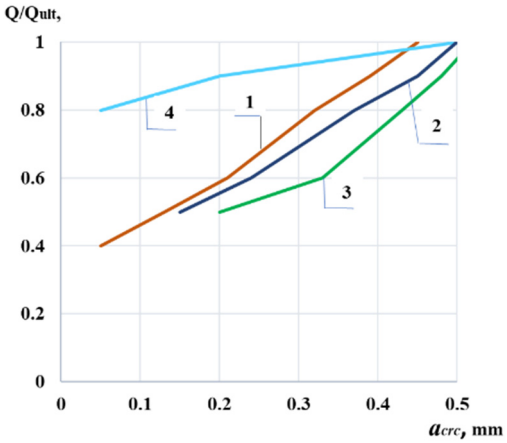


Figure 9. Width of opening of shear cracks in the BO specimen beam.

Cracking indicators at 3% steel fiber content were still considerably more than the control beam; though a slight decrease compared to the 2% series was also found. Such a reduction can be attributed to low workability at high fiber volume fractions which enhances the chances of fiber balling and irregular distribution. These effects can locally degrade the quality of cementitious matrix and weaken the fiber–matrix bond, and hence inhibit the action of fiber pull-out resistance and stress redistribution mechanisms. On the whole, the findings substantiate the claim that fiber reinforcement retards normal and inclined crack propagation as well as lessens crack dimensions during loads at service levels, whereas steel fibers offer the strongest enhancement in shear cracking and stability after cracking.

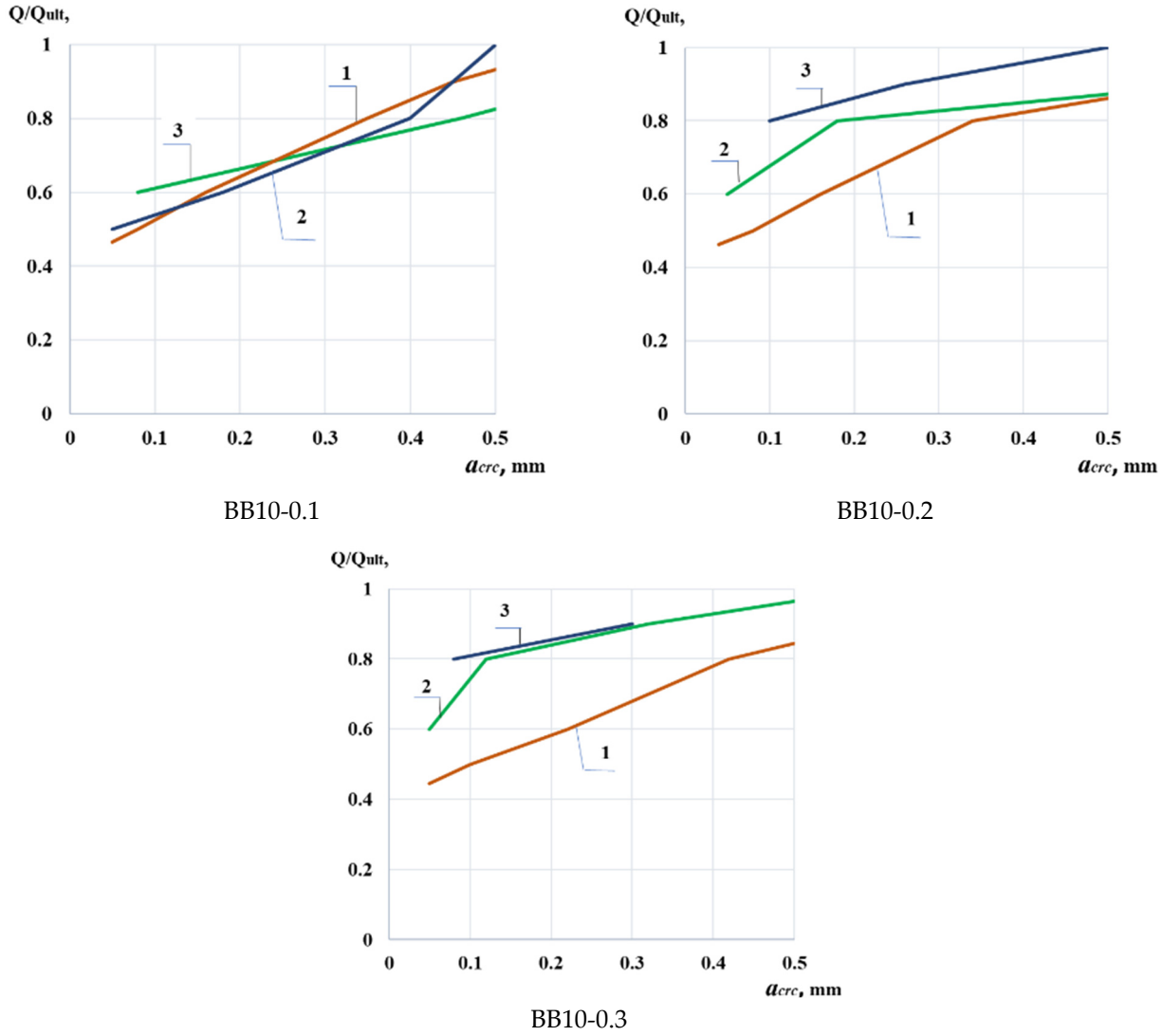


Figure 10. Width of opening of shear cracks in the sample beam S2.

Steel, basalt and polypropylene fibers significantly affected the crack resistance of reinforced concrete beams. Since steel fibers have a high modulus of elasticity and tensile strength, they act as bridges on the surface of cracks and effectively resist the expansion of cracks. The fibers continued to carry loads even after the formation of cracks, that is, they increased the strength of concrete in the initial crack formation. The overall crack resistance of the fiber-reinforced concrete beam was ensured. Basalt fibers also had an effective effect on increasing the crack resistance of concrete. They were distributed in the concrete before the formation of microcracks and participated in the distribution of forces. Basalt fibers ensured that the stresses during bending did not accumulate at one point, reducing the formation of microcracks. Polypropylene fibers limited the width of the cracks and reduced the number and size of cracks on the surface of the beam.

The relative deformations of the concrete in front of the support of fiber-reinforced concrete and reinforced concrete beams were measured using a measuring device installed along the inclined section. The deformations of the concrete along the inclined section did not have large values at the initial stages of loading, and their change increased almost linearly. When the load reached 60 ÷ 70 kN, the relative deformation of the BO-1 (plain concrete) sample reached $\varepsilon_{fb} = (2 \div 7) \times 10^{-4}$. In the BS30-1.0, BS30-2.0 and BS30-3.0 sample beams, that is, fiber-reinforced concrete samples with the addition of steel fibers,

the deformations remained relatively low. For example, the relative deformation of the BS30-1.0 sample under a load of 60 ÷ 70 kN was $\varepsilon_{fb} = (0.85 \div 1.05) \times 10^{-4}$.

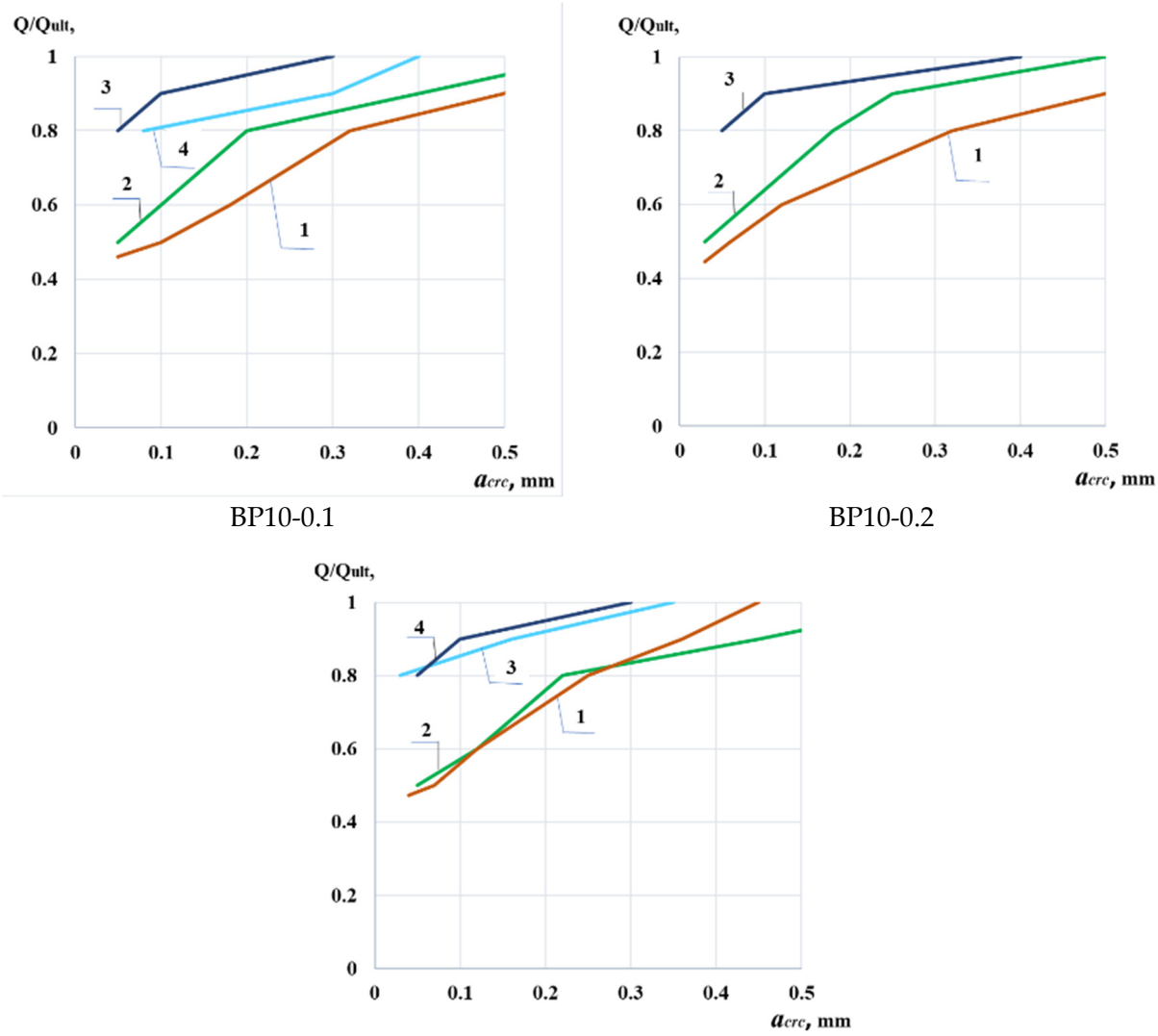


Figure 11. Width of opening of shear cracks in the sample beam S3.

As the load increased, especially when the breaking force in the oblique section reached 140 ÷ 150 kN, the relative deformations in the samples became much larger. In ordinary concrete, that is, in the BO-1 sample, the deformations at this stage increased to $\varepsilon_{fb} = (75 \div 80) \times 10^{-4}$. In the steel fiber-reinforced concrete samples, the deformations at this stage were relatively small. In the BS30-1.0 series sample, the relative deformation reached $\varepsilon_{fb} = (50 \div 60) \times 10^{-4}$, in the BS30-2.0 series sample, the relative deformation reached $\varepsilon_{fb} = (35 \div 50) \times 10^{-4}$, and in the BS30-3.0 series sample, the relative deformation reached $\varepsilon_{fb} = (65 \div 70) \times 10^{-4}$. The average relative deformation of concrete in beams dispersedly reinforced with steel fibers is presented in Figure 13.

The results of the experiment on fiber-reinforced concrete beams dispersedly reinforced with basalt fibers showed that the volume and length of the fibers significantly affected the relative deformations of concrete in the stages of loading in the oblique section. When adding 30 mm long basalt fibers to the concrete in an amount of 0.1%, the relative deformations of concrete in the oblique section reached the values $\varepsilon_{fb} = (1.25 \div 3.0) \times 10^{-4}$

when the breaking force in the oblique section reached 60 ÷ 70 kN in the dispersed reinforced fiber-reinforced concrete beams (Figure 14).

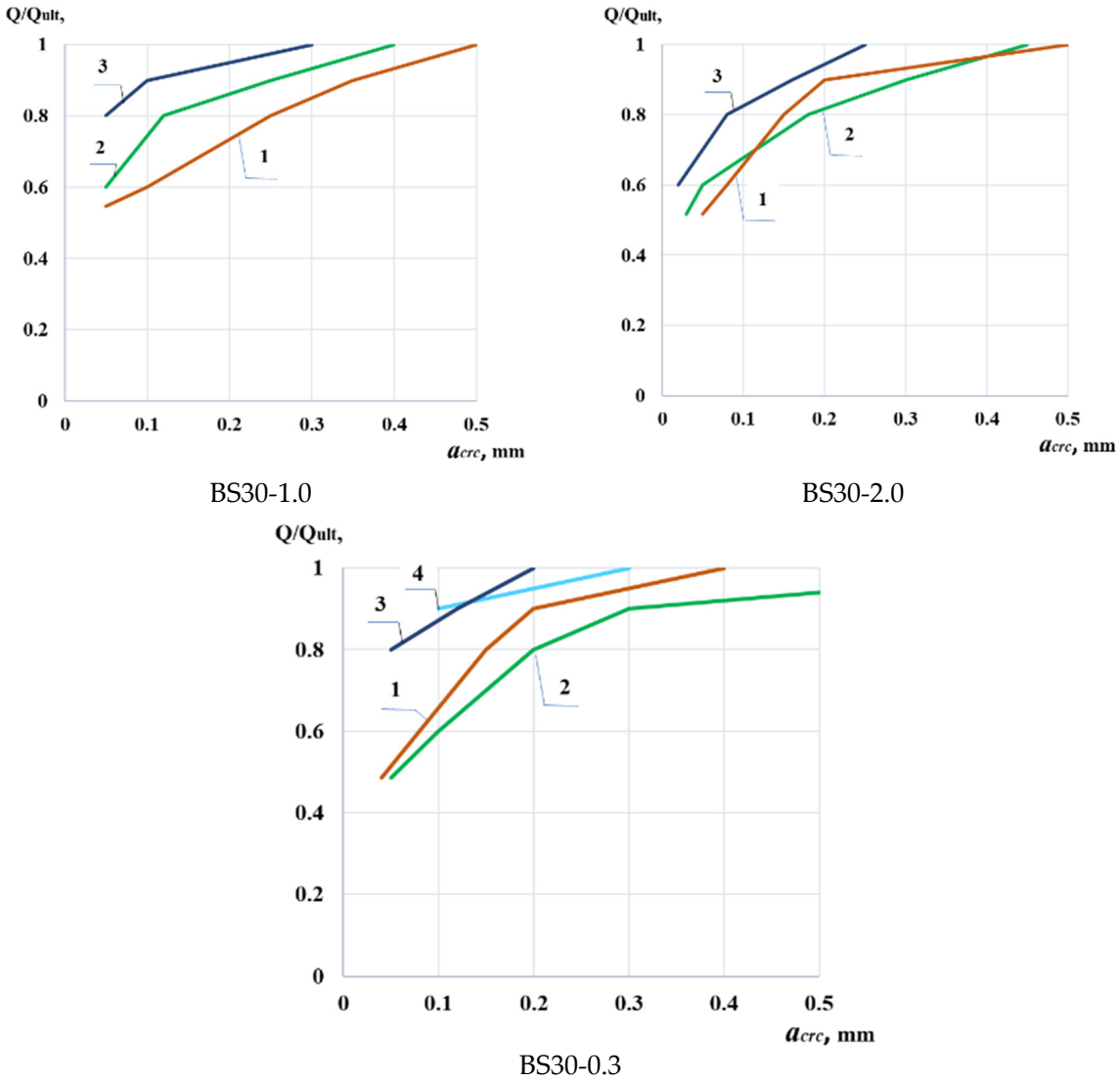


Figure 12. Width of opening of shear cracks in the sample beam S4.

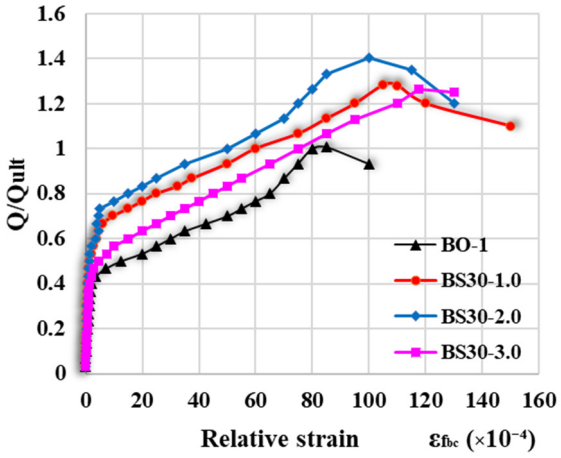


Figure 13. Relative strains of concrete for group 1 beams.

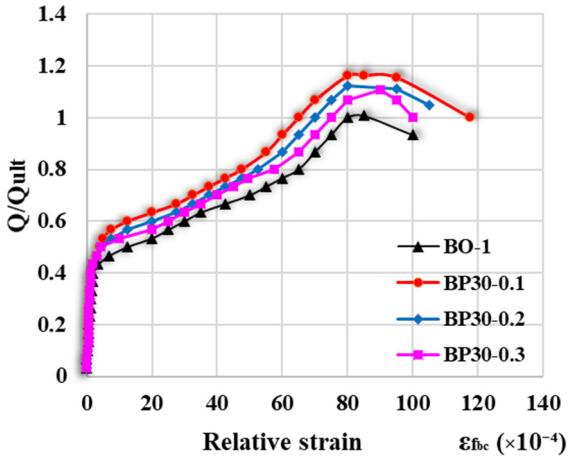


Figure 14. Relative strains of concrete for group 2 beams.

This indicator reached the values $\varepsilon_{fb} = (1.90 \div 3.3) \times 10^{-4}$ in fiber-reinforced concrete beams with dispersed reinforcement by adding 0.2% basalt fibers with a length of 30 mm to the concrete, and $\varepsilon_{fb} = (2.2 \div 3.6) \times 10^{-4}$ in fiber-reinforced concrete beams with dispersed reinforcement by adding 0.3% basalt fibers with a length of 30 mm to the concrete. When the breaking force along the slope reached 140 ÷ 150 kN, the relative deformations in the samples reached $\varepsilon_{fb} = (75 \div 80) \times 10^{-4}$ in ordinary concrete. The relative deformation in the BB30-0.1 series sample reinforced with basalt fibers reached the values $\varepsilon_{fb} = (60 \div 65) \times 10^{-4}$, in the BB30-0.2 series sample the relative deformation $\varepsilon_{fb} = (50 \div 58) \times 10^{-4}$, and in the BB30-0.3 series sample the relative deformation $\varepsilon_{fb} = (65 \div 70) \times 10^{-4}$.

In order to evaluate the deflection behavior of fiber-reinforced concrete beams, experiments were conducted under laboratory conditions. During the tests, reinforced concrete beams with dispersed reinforcement of different fiber contents and lengths were subjected to stepwise loading, and the corresponding deflections at each loading stage were measured.

In the initial stages of loading in samples with dispersed fiber reinforcement, the increase in deflection was close to that observed in the reference specimens. It was established that, when under loads of 20–70 kN, steel fiber-reinforced concrete had a better stiff-ness than the concrete with no fibers, which means that it has higher internal resistance of the building. This is the point whereby, particularly in samples that contained 2% and 3% of the fibers, the load versus deflection response built up steadily. The 3 percent steel fiber BS30-3.0 sample had predictable steady deflection behavior during most of the loading stages. As an illustration, the deflection of the BS30-3.0 sample was 0.470 mm at 25 kN, whereas the deflection of the BS30-2.0 sample was 0.418 mm, the deflection of the BS30-1.0 sample was 0.38 mm, and the deflection of the BO-0 sample was 0.3 mm (Figure 15).

When the value of the breaking force reached 60 kN, the deflection in the BS30-3.0 sample reached 1.8 mm, while in BS30-2.0 it was 1.5 mm, in BS30-1.0 it was 1.5 mm, and in BO-0 it was 2.1 mm. In reinforced concrete beams made of ordinary concrete, when the value of the breaking force reached 80 ÷ 90%, that is, (130 ÷ 140 kN), the deflection value was 10 ÷ 12 mm. At this loading stage, the deflection in BS30-3.0 was 8.8 mm, in BS30-2.0 it was 7.5 mm, and in BS30-1.0 it was 8.8 mm.

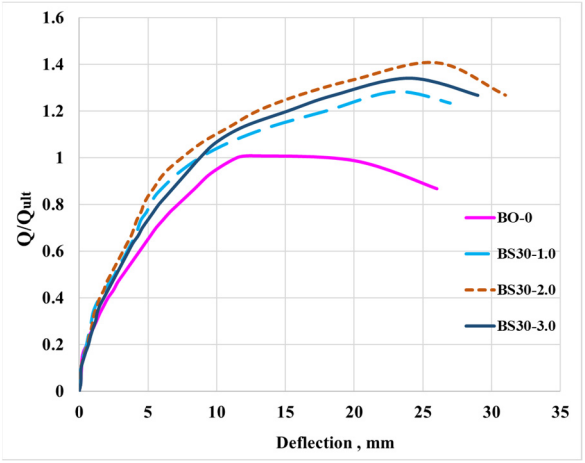


Figure 15. Concrete deflection for beams of group 1.

The deflection characteristics of concrete samples with the addition of polypropylene fibers (BP30-0.3, BS30-0.2, BS30-0.1) show that at stages with a breaking load of up to 60 kN in the transverse section, the deflection in the BP30-0.3 and BS30-0.2 samples showed a greater resistance by a difference of 0.2 ÷ 0.3 mm compared to the deflection of reinforced concrete beam samples made of ordinary concrete BO-0. For example, at 60 kN, the deflection in BO-0 was 2.1 mm, while in BS30-0.1 it was 1.4 mm, in BP30-0.3 it was 1.9 mm, and in BS30-0.2 it was 1.7 mm (Figure 16).

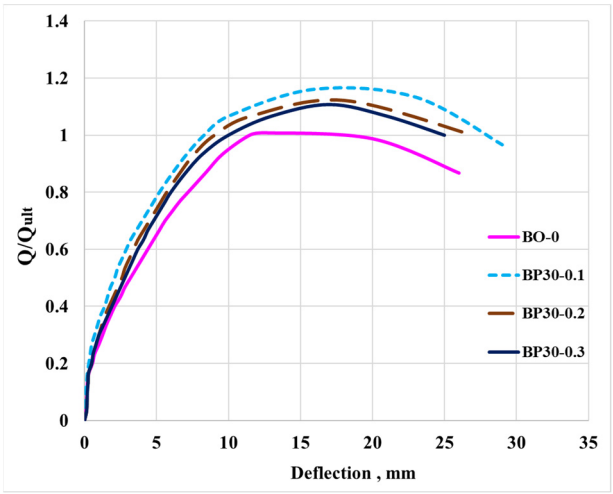


Figure 16. Concrete deflection for beams of group 2.

The transverse failure of beams with dispersed fiber reinforcement was significantly different from that of classical reinforced concrete beams. Dispersed reinforcement—that is, the addition of fibers distributed not in a single direction but in volume to the concrete mass—affected the failure processes in fiber-reinforced concrete beams under the influence of transverse forces. The transverse failure occurs mainly due to the formation and development of diagonal cracks in the internal structure of concrete as a result of increased transverse forces or large moments in the beam.

According to the results of scientific research, transverse failure in beams with dispersed reinforcement with steel, basalt, and polypropylene fibers occurs later, and the cracks develop at a smaller angle and more slowly. This can be explained by the fact that the fibers partially absorb the shear forces and disperse local stresses in the transverse section of concrete. In particular, since steel fibers have high elasticity and tensile strength, they act as a "bridge" between diagonal cracks, maintaining the load-bearing capacity of

the beam for a certain period of time. This is manifested not by brittle failure in the beam along the oblique section but by continuous plastic failure. The load-bearing capacity of the beams under shear is presented in Figure 17.

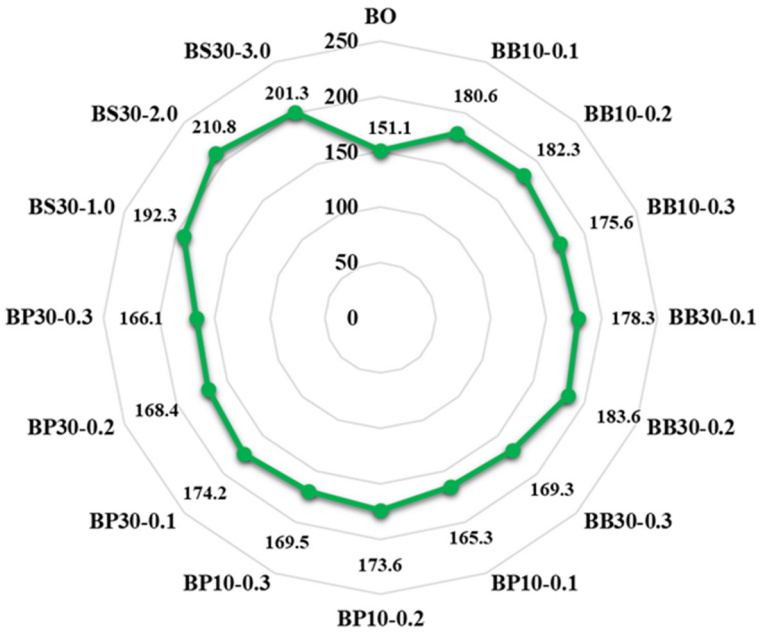


Figure 17. Load-bearing capacity of beams according to the shear.

The tensile strength and elastic modulus of basalt and polypropylene fibers are lower than these indicators of steel fibers. However, they are important in preventing microcracks that appear in the plastic state of concrete (before solidification). It was observed that they contribute not to the process of failure occurring in the oblique section but to the reduction in the initial internal defects—cracks that can create the basis for this failure.

Fibers increase aggregate interlocking and dowel action mechanisms. Fibers limit the crack opening and are used to hold the aggregates together as well as serve as dowels that transfer shear forces across the cracks. This means that the fiber-reinforced concrete beams are more shear-resistant and ductile in their mode of failure.

In fiber-reinforced concrete beams with the addition of fibers, cracks along the oblique section developed at a small angle, their width became smaller, and they spread in the form of several diagonal lines. After the cracks formed, the beam continued to carry the load for a certain period of time without losing its full strength.

3.2. Shearing Capacity of Fiber-Reinforced Concrete Beams

The strength of fiber-reinforced concrete beams in the shear section was calculated based on the requirements of SP 297.1325800.2017. The theoretical bearing capacity of a beam along a diagonal section is determined by the condition of equilibrium of all forces (external—Q and internal—$Q_{bf} + Q_{sw}$).

$$\sum Q = 0 \rightarrow Q_{theor} = Q_{bf} + Q_{sw} \quad (1)$$

Q_{bf}—the shear force supported by compressed fiber concrete above an oblique crack

$$Q_{bf} = \psi_2 \cdot R_{fb} \cdot b \cdot \frac{h_0^2}{c_0} \quad (2)$$

where ψ_2—coefficient; R_{fb}—design compressive strength of fiber concrete; b—beam width; h_0—effective depth; c_0—diagonal shear projection (mm) at the most critical diagonal cracking location.

Q_{sw}—shear force supported by transverse bars crossing an oblique crack

$$Q_{sw} = q_{sw} \cdot c_{sw} \tag{3}$$

$$q_{sw} = \frac{R_{sw} \cdot A_{sw}}{S} \tag{4}$$

where S—stirrup spacing; C_{sw}—diagonal section projection; R_{sw}—calculated resistance of transverse reinforcement; A_{sw}—cross-sectional area of the stirrup; q_{sw}—shear force in the stirrup.

The repeatability of the experimental results of the fiber-reinforced concrete beams was good. The average ultimate shear load of each beam series of three specimens ranged between 151.1 kN (control) and 210.8 kN (BS30-2.0) with the standard deviation ranging between 1.5 kN and 5.3 kN. The values of corresponding coefficient of variation (COV) were not more than 2.6, which means that there was relatively low scatter and that the measurements that were taken in the experiment were rather reliable. This means that the preparation and testing of the specimens were treated in the same manner in all the series. The fact that the COV values are low points to the even distribution of the fibers in the concrete matrix. The experimental findings therefore give a strong foundation on which the effects of the type of fiber, dose, and length can be evaluated on the shear performance.

The theoretical and experimental strength results for the shear section are presented in Table 5.

Table 5. Theoretical and experimental strength results for shear sections.

Series	ID	Q_{thear}, (kN)	Q_{exp}, (kN)	$\frac{Q_{exp}}{Q_{thear}}$
S1 (Control)	BO	144.6	151.1	0.95
S2	BB10-0.1	171.08	180.6	9.52
	BB10-0.2	174.61	182.3	7.69
	BB10-0.3	165.34	175.6	0.94
	BB30-0.1	164.46	178.3	0.92
	BB30-0.2	173.72	183.6	0.95
	BB30-0.3	167.99	169.3	0.99
S3	BP10-0.1	166.66	165.3	1.01
	BP10-0.2	168.87	173.6	0.97
	BP10-0.3	165.78	169.5	0.98
	BP30-0.1	169.75	174.2	0.97
	BP30-0.2	167.10	168.4	0.99
	BS30-0.3	164.02	166.1	0.99
S4	BS30-1.0	200.64	192.3	1.04
	BS30-2.0	203.28	210.8	0.96
	BS30-3.0	183.87	201.3	0.91

These findings show that the measured beams showed consistent results among specimens, which justifies the observed pattern of the effect of fiber type and content on shear capacity.

4. Discussion

It is certainly seen that the experiment results indicate that distributed fibers play a great role in determining the stress–strain behavior, crack development, and shear resistance of reinforced concrete beams under shear loading. The fracture mechanics point of view can

agree with the fact that the enhancement of performance is explained by the crack-bridging effect of fibers, which postpones the crack initiation, decreases the crack opening, and restricts unstable crack propagation. During tensile tests of fiber-reinforced specimens, tensile stresses are partially passed through cracks by fiber bridging, which leads to better post-cracking stiffness and energy dissipation than the control beams. In the case of a basalt fiber-reinforced concrete beam, compressive and tensile strength is seen to increase, especially at a fiber content of 0.2% and a length of 10 mm, since the stress transfer between the microcracks across the fiber is uniformly distributed. The thin fibers of basalt increase the interfacial bond between the cement matrix and cement load transfer and postpone the development of microcracks into macro-cracks. The decrease in performance at higher fiber contents is linked with lower workability and agglomeration of fibers when compared to lower fiber content, which is harmful to the homogeneity of the matrix and restricts the efficacy of the crack-bridging processes.

The increase in flexural strength and residual tensile strength realized in basalt fiber-reinforced beam is an indication of the increased energy absorption capacity and crack widening resistance. The fiber pull-out mechanism explains this response, where the basalt fibers, via a process of friction and mechanical anchorage, relay stresses across forming cracks, which decelerates the process of crack propagation and improves ductile behavior. There were moderate enhancements in strength and control of crack in polypropylene fiber-reinforced concrete beams. This is in line with the fact that polypropylene fibers have a lower ability of elasticity that limits their contribution to the weight-bearing capacity. Nonetheless, the polypropylene fibers are useful in controlling early cracking since they limit crack initiation and narrow crack widths when subjected to service loads. This decrease in the width of the diagonal cracks up to being half of the final shear load shows that the polypropylene fibers mainly contribute to high serviceability performance but not ultimate shear strength.

Improvements in shear cracking load, ultimate load, stiffness and crack control were the most pronounced on steel fiber-reinforced concrete beams. These improvements can be linked to the fact that steel fibers have a high tensile strength and elastic modulus which plays an important role in shear transfer of the fibers in the form of enhancement of aggregate interlocking, fiber bridging diagonal cracks, and enhanced dowel action of longitudinal reinforcement. The performance decrease with greater fiber content is insignificant enough to indicate the possibility of an optimal level of fiber dosage, beyond which fiber clustering and decreasing workability diminishes the usefulness of fiber pull-out resistance and stress redistribution mechanisms. Comprehensively, the findings suggest that the role of dispersed fibers in reducing shear resistance is regulated by a set of fracture mechanics, behavior on fiber pull-out, and shear transfer mechanisms. Depending on the mechanical characteristics, dosage, and dispersion in the concrete matrix, the effectiveness of each fiber type is crucial in shear-crashing reinforced concrete elements, which explains the significance of optimized fiber selection.

Once the steel fiber content reaches 3 percent, the concrete strength is lower than that of the 2 percent fiber content mainly because of the lower workability and the higher propensity of the fibers to cluster. Consequently, the cement paste does not entirely enter the interim between the fibers and results in high porosity in the concrete. It has been shown through experimental evidence that above 3 percent fiber content, the fibers do not evenly distribute, and thus the fibers are not able to transfer stress in the overall structure, leading to the ultimate weakening of the structure and decreasing the bond strength of the fibers and concrete.

5. Conclusions

This research examined the impacts of basalt, steel and polypropylene fiber-dispersed reinforcement in stress–strain behavior, crack development and load-bearing capacity of reinforced concrete beam. The most important findings are as follows:

1. The onset and propagation of oblique and normal cracks was greatly postponed with the use of fiber reinforcement. Where brittle failure of ordinary concrete beams occurred at the low loads, the introduction of fibers enabled the beams to maintain load-bearing capacity even after the cracks had been formed. Steel fibers were especially very successful and then were basalt and polypropylene fibers in bridging the cracks and controlling the width of the cracks.
2. Spread fibers enhanced weight carrying ability of beams in shear sections and minimized the chances of brittle failure of the beam that occurred abruptly. The basalt fibers contributed to the load capacity enhancement by 12–21 percent, polypropylene fibers by 9–15 percent, and steel fibers by 27–40 percent showing that fiber type, content and length appeared critical in increasing beam performance.
3. The fibers served as micro-distribution of tensile stresses and retardation of crack coalescence, by the micro-bridging of developing cracks. This multiscale reinforcement mechanism resulted in slower degradation of stiffness, increased post-cracking ductility, and increased loading-absorption energy. Steel fibers were the most significant bridging and it is because of their high tensile strength and modulus which makes it superior compared to basalt fibers which offered durability and sustainability.
4. The results substantiate that dispersed fiber reinforcement is a viable approach to improve the flexural and shear behavior of concrete beams especially in structures which are likely to be subjected to dynamic or high service loads. The choice of the type of fiber and dosage enables the engineer to balance the structural reliability and the service life and reduce the damage caused by cracks to the minimal.
5. In case of moderate improvement of shear resistance, basalt fibers of 0.1–0.3 percent by volume and polypropylene ones of the same dosages may be employed. To achieve the maximum shear capacity enhancement, the steel fibers with 1.0–3.0% volume are suggested.
6. Future studies should test the results at elevated temperatures. This will help to better understand how concrete and fiber mixtures behave under fire, the cracking and deformation processes, and the impact on the load-bearing capacity of the structure. This will allow the effectiveness of fiber type, length, and quantity in elevated temperatures to be evaluated and safe design recommendations to be developed.
7. The present study was conducted on small-scale beams under static loading. Tests of full-sized beam and with cyclic loading are done to further verify the findings.

Author Contributions: Conceptualization, A.M.; methodology, A.M.; validation, A.M. and S.R.; formal analysis, A.M.; investigation, A.M.; resources, A.M.; data curation, A.M.; writing—original draft preparation, A.M.; writing—review and editing, S.R.; visualization, A.M.; supervision, S.R.; project administration, A.M.; funding acquisition, A.M. All authors have read and agreed to the published version of the manuscript.

Funding: This research received no external funding.

Data Availability Statement: The original contributions presented in the study are included in the article, further inquiries can be directed to the corresponding author.

Conflicts of Interest: The authors declare no conflicts of interest.

References

1. Chia, E.; Nguyen, H.B.; Le, K.N.; Bi, K.; Pham, T.M. Performance of hybrid basalt-recycled polypropylene fibre reinforced concrete. *Structures* **2025**, *75*, 108711. [CrossRef]
2. Hassan, M.J. Effect of basalt macro fiber on shear strength of high-strength concrete beams with web openings: A finite element parametric study. *Case Stud. Constr. Mater.* **2025**, *23*, e05088. [CrossRef]
3. Liu, Q.; Cai, L.; Guo, R. Experimental study on the mechanical behaviour of short chopped basalt fibre reinforced concrete beams. *Structures* **2022**, *45*, 1110–1123. [CrossRef]
4. Sheikh, N.A.; Katkhuda, H.; Shatarat, N. Effect of 3D, 4D, 5D steel fibers on the shear behavior of reinforced concrete beams made of recycled coarse aggregate. *Constr. Build. Mater.* **2025**, *460*, 139842. [CrossRef]
5. Zheng, Y.; Zhang, Y.; Zhuo, J.; Zhang, Y.; Wan, C. A review of the mechanical properties and durability of basalt fiber-reinforced concrete. *Constr. Build. Mater.* **2022**, *359*, 129360. [CrossRef]
6. Vairagade, V.S.; Dhale, S.A. Hybrid fibre reinforced concrete–A state of the art review. *Hybrid Adv.* **2023**, *3*, 100035. [CrossRef]
7. Chen, X.-F.; Kou, S.-C.; Xing, F. Mechanical and durable properties of chopped basalt fiber reinforced recycled aggregate concrete and the mathematical modeling. *Constr. Build. Mater.* **2021**, *298*, 123901. [CrossRef]
8. Jiang, C.; Fan, K.; Wu, F.; Chen, D. Experimental study on the mechanical properties and microstructure of chopped basalt fibre reinforced concrete. *Mater. Des.* **2014**, *58*, 187–193. [CrossRef]
9. Vedhasakthi, K.; Chithra, R. Strength attributes and microstructural characterization of basalt fibre incorporated self-compacting concrete. *J. Build. Eng.* **2023**, *78*, 107592. [CrossRef]
10. Mousavi, S.S.; Dehestani, M. Influence of mixture composition on the structural behaviour of reinforced concrete beam-column joints: A review. *Structures* **2022**, *42*, 29–52. [CrossRef]
11. Ralegaonkar, R.; Gavali, H.; Aswath, P.; Abolmaali, S. Application of chopped basalt fibers in reinforced mortar: A review. *Constr. Build. Mater.* **2018**, *164*, 589–602. [CrossRef]
12. Shyamala, G. Impact of reinforcement and geometry of deep beam–Research perspective. *Mater. Today Proc.* **2022**, *68*, 1556–1561. [CrossRef]
13. Silva, D.B.; Pachla, E.C.; Bolina, F.L.; Graeff, Â.G.; Lorenzi, L.S.; da Silva Filho, L.C.P. Mechanical and chemical properties of cementitious composites with rice husk after natural polymer degradation at high temperatures. *J. Build. Eng.* **2024**, *85*, 108716. [CrossRef]
14. Shi, K.; Gao, Z.; Kang, L. Flexural behavior of steel fiber-reinforced recycled aggregate concrete beam reinforced with hybrid steel and FRP bars. *Structures* **2025**, *80*, 109665. [CrossRef]
15. Wang, H.; Zhou, M.; Wei, B.; Wu, C.; Tang, Z.; Zhang, S.; He, J. Study on flexural cracking characteristics of polypropylene fiber reinforced concrete beams with BFRP bars. *Case Stud. Constr. Mater.* **2025**, *22*, e04372. [CrossRef]
16. Shabani, H.; Asadian, A.; Galal, K. Flexural and serviceability behaviour of macro-synthetic fibre-reinforced concrete beams reinforced with GFRP bars. *Constr. Build. Mater.* **2025**, *494*, 143217. [CrossRef]
17. Lang, W.; Chen, W.; Xie, Q.; Wang, P.; Zhang, G. Flexural performance of basalt fiber reinforced recycled aggregate concrete subjected to sulfate corrosion. *Case Stud. Constr. Mater.* **2025**, *23*, e05156. [CrossRef]
18. Zhou, Y.; Xiao, J.; Deng, Z.; Yang, H.; Mei, J.; Huang, J. Experimental and modelling investigation of stress-strain behavior of basalt fiber-reinforced coral aggregate concrete under uniaxial and triaxial compression. *Constr. Build. Mater.* **2025**, *496*, 143856. [CrossRef]
19. Liu, Z.; Kong, D.; Wang, L.; Liu, A.; Xu, F.; Fang, Z.; Wang, S. Performance of red mud concrete reinforced with single and hybrid Polyvinyl alcohol and Basalt fibers. *J. Build. Eng.* **2025**, *112*, 113879. [CrossRef]
20. Wei, J.; Li, J.; Liu, Z.; Wu, C.; Liu, J. Behaviour of hybrid polypropylene and steel fibre reinforced ultra-high performance concrete beams against single and repeated impact loading. *Structures* **2023**, *55*, 324–337. [CrossRef]
21. Ye, Y.; Xie, T.; Guo, T.; Dong, B.; Zhao, J.; Feng, J. Durability evaluation and life prediction of basalt fiber reinforced aeolian sand concrete in different freeze-thaw media. *J. Build. Eng.* **2025**, *117*, 114924. [CrossRef]
22. Esakki, A.K.D.K.; Dev, S.K.A.; Gomathy, T.; Chella Gifta, C. Influence of adding steel–glass–polypropylene fibers on the strength and flexural behaviour of hybrid fiber reinforced concrete. *Mater. Today Proc.* 2023, *in press*. [CrossRef]
23. Yang, K.; Wu, Z.; Zheng, K.; Shi, J. Shear behavior of regular oriented steel fiber-reinforced concrete beams reinforced with glass fiber polymer (GFRP) bars. *Structures* **2024**, *63*, 106339. [CrossRef]
24. Mashayekhi, A.; Hassanli, R.; Zhuge, Y.; Ma, X.; Chow, C.W.K.; Bazli, M.; Manalo, A. Shear performance of fibre-reinforced seawater sea-sand concrete–fibre hybridization and synergy effects. *Constr. Build. Mater.* **2025**, *472*, 140955. [CrossRef]
25. Mirzaaghabeik, H.; Mashaan, N.S.; Shukla, S.K. Impact of geometrical dimensions on the shear behaviour of UHPC deep beams reinforced with steel and synthetic fibres. *Structures* **2025**, *78*, 109260. [CrossRef]
26. Yu, J.; Yufeng, X.; Saijie, L.; Zhiqiang, X. Experimental study on shear performance of basalt fiber concrete beams without web reinforcement. *Case Stud. Constr. Mater.* **2022**, *17*, e01602. [CrossRef]

27. Yan, X.; Wang, F.; Luo, Y.; Liu, X.; Yang, Z.; Mao, H. Mechanical performance study of basalt-polyethylene fiber reinforced concrete under dynamic compressive loading. *Constr. Build. Mater.* **2023**, *409*, 133935. [CrossRef]
28. He, L.; Wu, F.; Ma, Y.; Li, Z.; Chen, A.; Zhao, B.; Cao, J. Flexural performance of steel fiber reinforced MPCC beams: Experimental study and theoretical analysis. *Eng. Struct.* **2025**, *343*, 121018. [CrossRef]
29. Islam, S.U.; Waseem, S.A. An experimental study on mechanical and fracture characteristics of hybrid fibre reinforced concrete. *Structures* **2024**, *68*, 107053. [CrossRef]
30. Cai, B.; Chen, H.; Xu, Y.; Fan, C.; Li, H.; Liu, D. Study on fracture characteristics of steel fiber reinforced manufactured sand concrete using DIC technique. *Case Stud. Constr. Mater.* **2024**, *20*, e03200. [CrossRef]
31. Xiong, Z.; Li, H.; Pan, Z.; Li, X.; Lu, L.; He, M.; Li, H.; Liu, F.; Feng, P.; Li, L. Fracture properties and mechanisms of steel fiber and glass fiber reinforced rubberized concrete. *J. Build. Eng.* **2024**, *86*, 108866. [CrossRef]
32. Al-Rousan, E.T.; Khalid, H.R.; Rahman, M.K. Fresh, mechanical, and durability properties of basalt fiber-reinforced concrete (BFRC): A review. *Dev. Built Environ.* **2023**, *14*, 100155. [CrossRef]
33. Yousefi, M.; Khandestani, R.; Gharaei-Moghaddam, N. Flexural behavior of reinforced concrete beams made of normal and polypropylene fiber-reinforced concrete containing date palm leaf ash. *Structures* **2022**, *37*, 1053–1068. [CrossRef]
34. Azandariani, M.G.; Vajdian, M.; Asghari, K.; Mehrabi, S. Mechanical properties of polyolefin and polypropylene fibers-reinforced concrete–An experimental study. *Compos. Part C Open Access* **2023**, *12*, 100410. [CrossRef]
35. *GOST 10180-2012*; The Method of Determining the Accuracy of the Control Method. Standartinform: Moscow, Russia, 2018.
36. *DR297.1325800.2017*; Fiber Reinforced Concrete Structures and Precast Products with Non-Steel Fibers. Design Rules. Ministry of Construction: Moscow, Russia, 2017.

Disclaimer/Publisher's Note: The statements, opinions and data contained in all publications are solely those of the individual author(s) and contributor(s) and not of MDPI and/or the editor(s). MDPI and/or the editor(s) disclaim responsibility for any injury to people or property resulting from any ideas, methods, instructions or products referred to in the content.